

Crystal Structures of V_nO_{2n-1} ($2 \leq n \leq 7$)

HIROYUKI HORIUCHI, NOBUO MORIMOTO, AND
MASAYASU TOKONAMI

*The Institute of Scientific and Industrial Research,
Osaka University, Yamadakami, Suita, Osaka 565, Japan*

Received May 7, 1975; in revised form, December 12, 1975

The crystal structures of V_3O_5 , V_6O_{11} , and V_7O_{13} have been refined by the single crystal intensity data collected by a counter method, and the structural relationships of homologous series, V_nO_{2n-1} ($2 \leq n \leq 7$), have been discussed in detail.

The structures of the series consist of octahedra of VO_6 . The bond distances and angles of the octahedra VO_6 systematically change according to the distance from the crystallographic shear plane (*CSP*) in each structure. The V-V distances across the shared octahedral faces in the *CSP* are almost identical with 2.768 ~ 2.780 Å from V_4O_7 to V_7O_{13} . The V-V distances across the shared octahedral edges are largest (3.161 ~ 3.250 Å) in the *CSP* and gradually become smaller with the increase of the distance from the *CSP* and the smallest distances are 2.798 Å of V_7O_{13} .

When the composition approaches to V_2O_3 in the series, the octahedra of VO_6 show greater distortions and expansions, especially in the *CSP*, though the displacement of vanadium atoms from the center of octahedra is smaller compared with the phases with larger n values in the series.

Introduction

Since the introduction of the concept of homologous series by Magneli (1) on the molybdenum oxides, various kinds of such series have been found in metal oxides. They have been extensively investigated because of much interest on their crystallographic and physical properties.

The existence of discrete phases with general formula V_nO_{2n-1} ($4 \leq n \leq 8$) was first revealed by Andersson (2) by the X-ray powder method. On the basis of the structure of Ti_5O_9 (Andersson (3)), Andersson and Jahnberg (4) determined the relationship of lattices between M_nO_{2n-1} (M represents V and Ti) and rutile, and proposed structure models of M_nO_{2n-1} using their X-ray powder patterns. The structures of homologous series M_nO_{2n-1} ($4 \leq n \leq 8$) take the triclinic symmetry.

Crystallographic study on the homologous series of V_nO_{2n-1} ($3 \leq n \leq 8$) was made at room temperature by Horiuchi et al. (5) with

single crystals synthesized by a chemical transport method by Nagasawa (6). According to them, the homologous series of V_nO_{2n-1} ($4 \leq n \leq 8$) (\mathbf{a}_n , \mathbf{b}_n , and \mathbf{c}_n) can be systematically expressed by the following relations based on the parent rutile-type lattice (\mathbf{a}_r , \mathbf{b}_r , and \mathbf{c}_r)¹,

$$\begin{aligned}\mathbf{a}_n &= -\mathbf{a}_r + \mathbf{c}_r, \\ \mathbf{b}_n &= \mathbf{a}_r + \mathbf{b}_r + \mathbf{c}_r, \\ \mathbf{c}_n &= \frac{1}{2}(2n-1)(\mathbf{b}_r + \mathbf{c}_r).\end{aligned}\quad (1)$$

In these expressions, the \mathbf{a}_n and \mathbf{b}_n axes coincide with those by Andersson and Jahnberg (4), and the length of the \mathbf{c}_n axis changes as a function of the n -value. The cell dimensions of V_nO_{2n-1} are listed in Table I. Although V_3O_5 belongs to monoclinic symmetry ($P2_1/n$, Horiuchi et al. (5)), it can be expressed by a triclinic lattice with $2\mathbf{a}_3$, \mathbf{b}_3 , and \mathbf{c}_3 in Eq. (1). This will be discussed later in detail. Recently

¹ The transformation matrix between a_r , b_r , and c_r in Eq. (1) and a_1 , a_2 , and c of the conventional tetragonal cell of rutile (7) is (010/100/001).

TABLE I
THE CELL DIMENSIONS AND SPACE GROUPS OF V_nO_{2n-1}

V_nO_{2n-1}	Space group	$a(\text{Å})$	$b(\text{Å})$	$c(\text{Å})$	α°	β°	γ°
V_2O_3	$R\bar{3}c$	4.990		13.980			
V_3O_5	$P2_1/n$	10.004	5.040	9.854		137.9	
	$P2_1/n \rightarrow P\bar{1}$	5.601×2	6.990	13.850	42.1	71.9	109.0
V_4O_7	$P\bar{1}$	5.504	7.007	19.243	41.3	72.5	109.4
V_5O_9	$P\bar{1}$	5.470	7.005	24.669	41.4	72.5	109.0
V_6O_{11}	$P\bar{1}$	5.448	6.998	30.063	41.0	72.5	108.9
V_7O_{13}	$P\bar{1}$	5.439	7.005	35.516	40.9	72.6	109.0

Asbrink (8) reported the space group $P2_1/n$ or Pn for V_3O_5 in which the structure has no 2-fold screw axis, however, the detail of the structure has not been reported yet. The reflections $0k0$ with $k = 2n - 1$ have not been observed in the precession photographic works by Horiuchi et al. (5).

The crystal structures of V_4O_7 and V_5O_9 were precisely determined first by Horiuchi et al. (9, 10) and precise measurements of the changes of cell parameters and the refinements of the structures of M_4O_7 and M_5O_9 (M represents V and Ti) were carried out at room and lower temperatures by Marezio et al. (11-14). The refined structures indicate considerable displacements of atoms from the ideal structures proposed by Andersson and Jahnberg (4).

In this investigation, the crystal structures of V_3O_5 , V_6O_{11} , and V_7O_{13} have been precisely determined at room temperature using single crystals, and structural relationships of homologous series, V_nO_{2n-1} ($2 \leq n \leq 7$), have been discussed in detail.

Experimental

Small fragments of single crystals of V_3O_5 , V_6O_{11} , and V_7O_{13} synthesized by a chemical transport method by Nagasawa (6) were used for determinations of the cell dimensions and crystal structures. The crystal sizes, maximum values of μr used for intensity collection and number of reflections used for structure analyses are $0.15 \times 0.15 \times 0.09$ mm, 0.66, 567 ($0 < \sin \theta / \lambda \lesssim 0.60$) for V_3O_5 , $0.15 \times 0.09 \times$

0.04 mm, 0.65, 1560 ($0 < \sin \theta / \lambda \lesssim 0.65$) for V_6O_{11} and $0.04 \times 0.12 \times 0.06$ mm, 0.51, 1434 ($0 < \sin \theta / \lambda \lesssim 0.60$) for V_7O_{13} , respectively.

The cell dimensions of V_nO_{2n-1} ($3 \leq n \leq 7$) were obtained by Horiuchi et al. (5). Those of V_2O_3 were determined based on the three reflections, 660, 060, and 0018 which were obtained by the Rigaku four-circle goniometer. The standard deviations of the cell dimensions of V_2O_3 are ± 0.001 Å and ± 0.002 Å for a and c , respectively.

All intensities were collected by the Rigaku four-circle automatic diffractometer by the $2\theta - \omega$ scan technique. Zr-filtered MoK α radiation was used.

Derivation of the Ideal Structures

For the structures of V_nO_{2n-1} the expressions of lattices by Horiuchi et al. (5) have been used in this work. The starting atomic parameters x_i , y_i , and z_i in the triclinic lattices are derived by the following relations similar to Eq. (1),

$$\begin{aligned} x_i &= y_r + z_r \\ y_i &= x_r - y_r + z_r \\ z_i &= \frac{2}{2n-1}(-x_r + 2y_r - z_r) + \frac{1}{2(2n-1)}, \end{aligned} \quad (2)$$

where x_r , y_r , and z_r are the atomic coordinates of the rutile structures. The final term, $1/2(2n-1)$, is introduced to coincide the origins of the structures of all the homologous series.

The rutile structure belongs to space group $P4_2/mnm$. The relationships of Eq. (2) were applied for vanadium and oxygen atoms at positions (2a) and (4g), respectively. The positions (2a) has equivalent sites of 0, 0, 0 and $\frac{1}{2}, \frac{1}{2}, \frac{1}{2}$, and (4g), $x_r, \bar{x}_r, 0, \bar{x}_r, x_r, 0, \frac{1}{2} + x_r, \frac{1}{2} + x_r, \frac{1}{2}$ and $\frac{1}{2} - x_r, \frac{1}{2} - x_r, \frac{1}{2}$. The value of 0.305 was used for x_r , which was determined for the high temperature form of VO_2 by Westman (15). Among the values calculated by the Eq. (2) using the above coordinates and their translated ones, the atomic coordinates of $0 \leq x_i < 1, 0 \leq y_i < 1$ and $0 \leq z_i < 1$ are

TABLE II(a)
FINAL ATOMIC PARAMETERS OF V_3O_5

Atoms	x	y	z	B
V1A	.15937(33)	.74408(47)	.27888(34)	.33(4)
V1B	.65960(33)	.24614(47)	.27887(33)	.32(4)
V20	.24832(33)	.25201(47)	.50088(34)	.35(4)
O1A	.2138(15)	.5929(21)	.1611(15)	1.13(15)
O1B	.7210(13)	.0962(17)	.1608(12)	.30(15)
O2A	.1140(13)	.9071(19)	.4398(13)	.56(17)
O2B	.6100(13)	.4053(19)	.4417(14)	.66(17)
O30	.0024(14)	.4440(20)	.2509(14)	.77(11)

TABLE II(b)

COMPARISON OF THE FINAL COORDINATES (x, y, z) AND THE IDEAL ONES (x_i, y_i, z_i)

Atoms	Ideal		Refined parameters (x, y, z) and ideal z_i coordinates			
	x_i	y_i	V_3O_5		V_6O_{11}	V_7O_{13}
V1	x	.0	.01184	.00772	-.00506(68)	-.00252(83)
	y	.5	.47198	.46739	.44815(78)	.45066(94)
	z		.12457	.12687	.06207(18)	.05220(18)
	B		.32	.32	.23(2)	.33(3)
	z_i		.1	.1	.045	.038
V2	x	.0	-.01184	-.00772	-.02670(68)	-.02908(83)
	y	.0	-.05170	-.04805	-.07425(77)	-.07677(95)
	z		.13641	.13459	.06734(18)	.05763(19)
	B		.33	.32	.19(2)	.35(3)
	z_i		.1	.1	.045	.038
V3	x	.0	.00402	-.00402	-.03621(70)	-.03877(83)
	y	.5	.49979	.50021	.45742(80)	.45346(94)
	z		.50054	.49946	.24248(18)	.20618(18)
	B		.35	.35	.31(2)	.32(3)
	z_i		.5	.5	.227	.192
V4	x	.0	-.00402	.00402	-.04519(70)	-.04913(84)
	y	.0	-.00825	.00825	-.05395(79)	-.06302(95)
	z		.50456	.49544	.24331(81)	.20821(19)
	B		.353	.353	.29(2)	.36(3)
	z_i		.5	.5	.227	.192
V5	x	.0			-.02496(72)	-.03579(85)
	y	.5			.46771(82)	.45384(96)
	z				.41727(19)	.35639(19)
	B				.40(2)	.41(3)
	z_i				.409	.346
V6	x	.0			-.01866(71)	-.02066(84)
	y	.0			-.02304(81)	-.02454(96)
	z				.41532(19)	.35202(19)
	B				.35(3)	.38(3)
	z_i				.409	.346

TABLE II(b) (continued)

Atoms	Ideal		Refined parameters (x, y, z) and ideal z_i coordinates			
	x_i and y_i coordinates		V_3O_5		V_6O_{11}	V_7O_{13}
V7	x	.0				.0
	y	.5				.5
	z					.5
	B					.43(3)
	z_i					.5
V8	x	.0				.0
	y	.0				.0
	z					.5
	B					.36(3)
	z_i					.5
O1	x	.695	.6893	.6858	.6939(28)	.6889(34)
	y	.390	.4111	.3977	.4177(32)	.4124(38)
	z		.0736	.0813	.03280(74)	.02784(75)
	B		.66	.56	.29(10)	.46(10)
	z_i		.066	.066	.030	.025
O2	x	.305	.3142	.3076	.3196(31)	.3196(34)
	y	.610	.5476	.5265	.5560(35)	.5594(39)
	z		.1457	.1564	.06693(82)	.05591(75)
	B		1.13	.30	.73(12)	.47(10)
	z_i		.134	.134	.061	.052
O3	x	.695	.6858	.6893	.6845(30)	.6831(33)
	y	.5	.4740	.4675	.4672(34)	.4646(38)
	z		.2329	.2371	.10880(78)	.09284(74)
	B		.56	.66	.51(11)	.43(10)
	z_i		.222	.222	.101	.085
O4	x	.305	.3880	.3880	.3743(29)	.3666(34)
	y	.5	.6418	.6342	.6208(33)	.6095(39)
	z		.3045	.3074	.14527(76)	.12549(76)
	B		.77	.77	.38(11)	.52(11)
	z_i		.378	.378	.172	.145
O5	x	.695	.6924	.6858	.6983(29)	.3666(34)
	y	.390	.4112	.4193	.4130(33)	.4085(40)
	z		.4640	.4598	.21149(76)	.18020(78)
	B		.30	.30	.42(11)	.63(11)
	z_i		.466	.466	.212	.179
O6	x	.305			.3137(30)	.3121(34)
	y	.610			.5890(34)	.5912(38)
	z				.24710(78)	.20865(75)
	B				.52(11)	.45(10)
	z_i				.242	.205
O7	x	.695			.6677(29)	.6659(34)
	y	.5			.4465(32)	.4464(39)
	z				.29735(75)	.25189(75)
	B				.35(10)	.48(10)
	z_i				.282	.239

TABLE II(b) (continued)

Atoms	Ideal		Refined parameters (x, y, z) and ideal z_i coordinates		
	x_i and y_i coordinates		V_3O_5	V_6O_{11}	V_7O_{13}
O8	x	.305		.3131(30)	.3208(34)
	y	.5		.5928(34)	.5357(39)
	z			.34820(78)	.29412(76)
	B			.53(10)	.49(10)
	z_i			.353	.299
O9	x	.695		.7079(30)	.7016(35)
	y	.390		.4271(34)	.4175(39)
	z			.38849(78)	.33115(77)
	B			.48(11)	.62(11)
	z_i			.394	.333
O10	x	.305		.3164(29)	.3066(35)
	y	.610		.5962(32)	.5915(40)
	z			.42607(75)	.36205(78)
	B			.35(10)	.66(11)
	z_i			.425	.359
O11	x	.695		.6903(30)	.6813(35)
	y	.5		.4721(34)	.4656(40)
	z			.47108(78)	.40000(78)
	B			.62(11)	.64(11)
	z_i			.465	.393
O12	x	.305			.3143(34)
	y	.5			.5279(39)
	z				.44830(76)
	B				.54(11)
	z_i				.453
O13	x	.695			.6950(34)
	y	.390			.4092(39)
	z				.48466(76)
	B				.52(11)
	z_i				.487

Atomic coordinates of V_3O_5 are converted into those by the triclinic cell.

adopted as starting atomic coordinates of V_nO_{2n-1} . The structures derived by Eq. (2) are called "ideal structures" in this work. The coordinates of the ideal structures are listed in Table II(b) by x_i , y_i , and z_i . The structural relation between V_3O_5 and other phases are explained later in detail.

Vanadium atoms of the ideal structures have the atomic coordinates of $x=0$, and $y=0$ and $\frac{1}{2}$. The symbols of V1, V3, V5, ..., are given to the vanadium atoms with $y = \frac{1}{2}$, and

V2, V4, V6, ..., to those with $y=0$ by the increasing order of the distance from the origin, respectively. Oxygen atoms are similarly called O1, O2, O3, ..., by the distance from the origin. The structure of V_6O_{11} is a combination of the structure of V_5O_9 and additional vanadium and oxygen atoms. The additional part has the rutile-type structure. The structure of V_7O_{13} can be obtained similarly from V_6O_{11} . The ideal structures in this study are essentially identical to "ideal"

ones proposed by Andersson and Jahnberg (4) except for O1. O1 atoms have the ideal atomic coordinates of $x = 0.695$ and $y = 0.390$, and $z = 0.047, 0.037, 0.030$, and 0.025 for $V_4O_7, V_5O_9, V_6O_{11}$, and V_7O_{13} , respectively, in this study. However, Andersson and Jahnberg gave $x = 0.695$ and $y = 0.500$, and $z = 0.016, 0.013, 0.010$, and 0.009 to the corresponding ones from V_4O_7 to V_7O_{13} .

The atomic coordinates of V_3O_5 in the monoclinic cell are converted into those in the triclinic cell by the following relations,

$$\begin{aligned} x' &= -y_m + 1, \\ y &= -2x_m - 2y_m + z_m + 2, \\ z &= x_m + y_m - z_m - \frac{1}{2}, \end{aligned} \quad (3)$$

where, x_m, y_m , and z_m are the atomic coordinates in the monoclinic cell and x', y and z in the triclinic cell. The constant terms are introduced to coincide the origin of the triclinic cell with that of other phases of V_nO_{2n-1} ($4 \leq n \leq 7$). The triclinic cell of V_3O_5 , thus obtained, however, has the a_3 axis twice longer than that in Eq. (1) and the center of symmetry is located at the $\frac{1}{2}a_3$ from the origin along the a_3 axis. The triclinic cell must, therefore, be divided into two cells along the a_3 axis and x' coordinates derived from Eq. (3) must be transformed by the following relations to compare with the other phases of the series;

$$\begin{aligned} x &= (x' - \frac{1}{2}) \times 2: \text{ for the lower-half part,} \\ x &= (x' - \frac{3}{2}) \times 2: \text{ for the upper-half part.} \end{aligned}$$

The right and left columns of the atomic coordinates for V_3O_5 in Table II(b) correspond to the lower-half and upper-half parts of the unit cell, respectively.

Structure determinations and refinements

The starting values of x and y coordinates of V_6O_{11} were derived from the results of V_5O_9 by Horiuchi et al. (10). In order to obtain z coordinates of V_6O_{11} from those of V_5O_9 , the ratio of the c length between V_5O_9 and V_6O_{11} was used. As for the additional vanadium and oxygen atoms in V_6O_{11} , the ideal atomic positions derived from Eq. (2) were used. In the same way, the refined structure of V_6O_{11} was used for V_7O_{13} . This method

resulted in a rapid convergence of the R values, especially for V_nO_{2n-1} with large values of n .

The refinement of the structure of V_3O_5 was initiated from the positional parameters given by Asbrink et al. (16).

Isotropic temperature factors of 0.30 \AA^2 were used as the starting values for both vanadium and oxygen atoms. Atomic scattering factors of V^{3+}, V^{4+} by Fukamachi (17) and O^{2-} by Tokonami (18) were used. The scattering factors of V^{3+} were applied to V1 and V2, and those of V^{4+} , to other vanadium atoms. However, this assignment does not necessarily mean the ordering of V^{3+} and V^{4+} in the structure.

The function minimized in the refinements was $\sum 1/\sigma_{hkl}^2 (s|Fo| - |Fc|)^2$, where σ_{hkl} is the value given by the counting statistics when $|Fo| \neq 0$, and 10.0 when $|Fo| = 0$, and s is the scale factor. Only the final refinements were carried out using unit weight for all reflections. The procedure of refinement was identical for all phases. The first several cycles of the least-squares refinement were carried out by varying only the positional coordinates and scale factor, and a few cycles were followed with the change of the positional parameters and the isotropic temperature factors. Finally, the atomic coordinates and the isotropic temperature factors were refined using unit weight for all reflections. In this final stage, the parameter for the secondary extinction effects was refined by the trial and error method using the equation by Zachariasen (19). A modified version of ORFLS (20) was used for refinements.

The R values for all reflections are 0.099, 0.093 and 0.098 for V_3O_5, V_6O_{11} , and V_7O_{13} , respectively, and those for nonzero reflections, 0.089, 0.086, and 0.088, respectively. The estimated secondary extinction parameter C 's are 9.5×10^{-6} , 7.0×10^{-6} , and 3.0×10^{-6} , respectively. Fo and Fc tables are deposited.² The final atomic coordinates and temperature

² See NAPS documents No 02745 for 24 pages of supplementary material. Order from ASIS/NAPS, c/o Microfiche Publications, 440 Park Avenue South, New York, N.Y. 10016. Remit in advance for each NAPS accession number \$3.00 for microfiche or \$6.00 for photocopies. Make checks payable to Microfiche Publications.

TABLE III

THE POSITIONAL SHIFTS OF ATOMS FROM IDEAL POSITIONS

Atoms	V_3O_5		$V_4O_7^*$	$V_5O_9^*$	V_6O_{11}	V_7O_{13}
V1	+++ .287	+++ .288	--- .300	--- .298	--- .316	--- .322
V2	--- .287	--- .288	--- .294	--- .289	--- .327	--- .335
V3	+++ .026	+- .026	--- .107	--- .154	--- .205	--- .217
V4	--- .027	+- .027	--- .109	--- .161	--- .177	--- .207
V5				—	--- .080	--- .115
V6				—	--- .063	--- .071
V7						—
V8						—
O1	--- .241	+++ .250	--- .237	--- .230	--- .237	--- .246
O2	+- .366	+- .420	+- .364	+- .328	+- .329	+- .320
O3	--- .083	--- .130	--- .114	--- .120	--- .115	--- .131
O4	+- .379	+- .350	+- .309	+- .290	+- .297	+- .259
O5	+- .136	+- .189	+- .163	+++ .148	+- .144	+++ .165
O6			--- .238	+- .157	+- .149	+- .128
O7			--- .197	--- .170	--- .194	--- .181
O8				+- .128	+- .105	+- .105
O9				+- .153	+- .127	+- .128
O10					+- .121	+- .094
O11					--- .111	--- .109
O12						+- .087
O13						+- .104

The directions of shifts are shown by + or - along a , b , and c axes, respectively. Numbers are the magnitudes (Å) of deviations from ideal positions. *-marked atomic coordinates (x, y, z) for V_4O_7 and V_5O_9 were obtained by the matrixes $(x/y/z) = (1, 0, 4/0, 1, 5/0, 0, -2)(x_M/y_M/z_M) + (\frac{1}{2}/\frac{1}{2}/\frac{1}{2})$ and $(x/y/z) = (1, 0, 2/0, 1, 3/0, 0, -1)(x_M/y_M/z_M) + (0/\frac{1}{2}/\frac{1}{2})$, respectively. Where, x_M , y_M , and z_M are atomic coordinates given by Marezio et al. (13, 14).

TABLE IV

COMPARISON OF THE V-O DISTANCES

Octahedra	Bonded oxygen		V_3O_5		V_6O_{11}	V_7O_{13}	
V1	O1a	O2A	2.11	O2B	2.16	2.11	2.13
	O1f	O2B ₀₆	2.11	O2A ₀₆	2.02	1.95	1.95
	O2	O1A	1.78	O1B	1.83	1.78	1.75
	O3a	O2B ₁₆	1.99	O2A ₁₁	2.01	1.96	1.97
	O4g	O30	2.05	O30 ₁₁	2.08	2.10	2.11
	O6c	O1A ₁₆	1.98	O1B ₁₂	1.96	1.87	1.86
	Mean		1.99		2.01	1.96	1.96
V2	O1f	O2B ₀₆	1.99	O2A ₀₆	2.01	2.00	2.00
	O2f	O1A ₀₆	1.98	O1B ₀₇	1.96	1.95	1.95
	O3c	O2B ₁₇	2.11	O2A ₁₃	2.02	1.96	1.95
	O3f	O2A ₂₄	2.11	O2B ₂₀	2.16	2.13	2.14
	O4c	O30 ₂₄	2.05	O30 ₀₆	2.08	2.01	2.00
	O5c	O1A ₂₄	1.78	O1B ₂₀	1.83	1.74	1.75
Mean		1.99		2.01	1.97	1.97	
V3	O1b	O2B ₀₃	2.03	O2A ₀₄	2.00	2.08	2.06
	O4	O30 ₀₉	2.02	O30 ₂₁	2.05	2.05	2.05
	O5a	O1A ₂₅	2.06	O1B ₂₂	1.95	2.00	1.99
	O6	O1B ₁₈	1.95	O1A ₁₄	2.06	1.93	1.90
	O7a	O30 ₁₉	2.05	O30 ₀₁	2.02	1.86	1.86
	O10c	O2A ₁₀	2.00	O2B ₀₈	2.03	1.88	1.86
Mean		2.02		2.02	1.97	1.96	
V4	O2	O1A	2.06	O1B	1.95	2.08	2.11
	O3	O2A ₁₁	2.00	O2B ₁₅	2.03	2.03	2.02
	O4	O30 ₀₉	2.05	O30 ₂₁	2.02	2.04	2.03
	O7c	O30 ₁₆	2.02	O30 ₀₅	2.05	1.91	1.91
	O8c	O2B ₂₅	2.03	O2A ₂₃	2.00	1.89	1.86
	O9c	O1B ₀₈	1.95	O1A ₀₆	2.06	1.85	1.84
	Mean		2.02		2.02	1.97	1.96
V5	O5b				2.06	2.05	
	O8				1.93	1.94	
	O9a				1.95	1.93	
	O10				1.98	1.95	
	O11a				1.90	1.91	
	O13i				O9i	1.95	1.86
	Mean					1.96	1.94
V6	O6				1.99	1.99	
	O7				1.96	1.95	
	O8				1.95	1.96	
	O11c				1.91	1.92	
	O12c				O11i	1.94	1.90
	O13c				O10i	1.93	1.93
	Mean					1.95	1.94

TABLE IV (continued)

Octahedra	Bonded oxygen	V_3O_5	V_6O_{11}	V_7O_{13}
V7	O9 <i>b</i>			1.98
	O12			1.92
	O13 <i>a</i>			1.95
	O9 <i>i</i>			1.98
	O12 <i>e</i>			1.92
	O13 <i>d</i>			1.95
	Mean			1.95
V8	O10			1.97
	O11			1.93
	O12			1.93
	O10 <i>i</i>			1.97
	O11 <i>i</i>			1.93
	O12 <i>i</i>			1.93
	Mean			1.94

The relations of symbols for oxygen atoms between V_7O_{13} and other phases are also shown. The suffix of italic and numerical letters are symmetry operation codes. Standard errors are around 0.01 Å for each phase.

SYMMETRY OPERATIONS

Monoclinic phase V_3O_5				Triclinic phase V_nO_{2n-1} ($4 \leq n \leq 7$)			
Symbols	Symmetry operations			Symbols	Symmetry operations		
None	<i>x</i>	<i>y</i>	<i>z</i>	None	<i>x</i>	<i>y</i>	<i>z</i>
01	<i>x</i>	<i>y</i>	$-1+z$	<i>a</i>	$-1+x$	<i>y</i>	<i>z</i>
02	$1+x$	$-1+y$	<i>z</i>	<i>b</i>	<i>x</i>	$1+y$	<i>z</i>
03	$-1+x$	<i>y</i>	$-1+z$	<i>c</i>	$-1+x$	$-1+y$	<i>z</i>
04	<i>x</i>	$-1+y$	$-1+z$	<i>d</i>	$1-x$	$1-y$	$1-z$
05	$1+x$	<i>y</i>	<i>z</i>	<i>e</i>	$-x$	$1-y$	$1-z$
06	$1-x$	$1-y$	$1-z$	<i>f</i>	$1-x$	$1-y$	$-z$
07	$2-x$	$-y$	$-z$	<i>g</i>	$1-x$	$2-y$	$-z$
08	$1-x$	$1-y$	$-z$	<i>h</i>	$-x$	$1-y$	$-z$
09	$-x$	$1-y$	$-z$	<i>i</i>	$-x$	$-y$	$1-z$
10	$-x$	$2-y$	$-z$	<i>j</i>	$-x$	$-y$	$-z$
11	$\frac{1}{2}-x$	$-\frac{1}{2}+y$	$\frac{1}{2}-z$				
12	$\frac{3}{2}-x$	$\frac{1}{2}+y$	$\frac{1}{2}-z$				
13	$\frac{3}{2}-x$	$-\frac{1}{2}+y$	$\frac{3}{2}-z$				
14	$\frac{1}{2}-x$	$-\frac{1}{2}+y$	$-\frac{1}{2}-z$				
15	$\frac{3}{2}-x$	$-\frac{1}{2}+y$	$\frac{1}{2}-z$				
16	$\frac{1}{2}-x$	$\frac{1}{2}+y$	$\frac{1}{2}-z$				
17	$\frac{3}{2}-x$	$\frac{1}{2}+y$	$\frac{3}{2}-z$				
18	$\frac{1}{2}-x$	$\frac{1}{2}+y$	$-\frac{1}{2}-z$				
19	$-\frac{1}{2}-x$	$\frac{1}{2}+y$	$-\frac{1}{2}-z$				
20	$\frac{1}{2}+x$	$\frac{1}{2}-y$	$\frac{1}{2}+z$				
21	$\frac{1}{2}+x$	$\frac{1}{2}-y$	$-\frac{1}{2}+z$				
22	$-\frac{1}{2}+x$	$\frac{1}{2}-y$	$-\frac{1}{2}+z$				
23	$\frac{1}{2}+x$	$\frac{3}{2}-y$	$-\frac{1}{2}+z$				
24	$\frac{1}{2}+x$	$\frac{3}{2}-y$	$\frac{1}{2}+z$				
25	$-\frac{1}{2}+x$	$\frac{3}{2}-y$	$-\frac{1}{2}+z$				
26	$\frac{3}{2}+x$	$-\frac{1}{2}-y$	$-\frac{1}{2}+z$				
27	$1-x$	$2-y$	$1-z$				
28	<i>x</i>	$-1+y$	<i>z</i>				

TABLE V
COMPARISON OF THE O-O DISTANCES AND O-V-O ANGLES

	Bonded oxygens	V_3O_5				V_6O_{11}		V_7O_{13}		
		O-O	O-V-O	O-O	O-V-O	O-O	O-V-O	O-O	O-V-O	
V1 octahedra	O1a-O1f	2.59 Å	77.6°	2.59 Å	76.4°	2.51 Å	76.3°	2.54 Å	76.8°	<i>e</i>
	O1a-O3a	2.58	77.9	2.58	76.4	2.57	78.9	2.59	78.1	<i>f</i>
	O1a-O4g	2.66	79.5	2.67	78.0	2.63	77.2	2.64	76.8	<i>f</i>
	O1a-O6c	2.72	83.0	2.71	82.2	2.69	84.5	2.67	83.7	<i>e</i>
	O1f-O2	2.86	97.9	2.93	98.7	2.86	100.1	2.85	100.1	
	O1f-O4g	2.71	83.9	2.72	82.9	2.67	82.3	2.68	82.4	<i>e</i>
	O1f-O6c	2.95	95.4	2.98	96.7	2.88	97.7	2.87	97.4	
	O2-O3a	3.02	106.5	3.12	108.5	2.96	104.4	2.93	103.9	
	O2-O4g	2.93	99.9	3.04	101.6	2.92	97.5	2.93	98.2	
	O2-O6c	2.84	97.9	2.87	98.5	2.82	100.9	2.80	101.4	
	O3a-O4g	2.67	84.6	2.66	81.1	2.65	81.3	2.66	81.5	<i>f</i>
	O3a-O6c	2.83	90.7	2.81	90.0	2.73	90.8	2.72	90.5	
	O1a-O2		175.5		175.0		173.9		174.4	
	O1f-O3a		153.8		150.8		152.0		152.7	
O4g-O6c		162.2		159.7		161.3		160.0		
Mean	2.78		2.81		2.74		2.74			
V2 octahedra	O1f-O2f	2.83	90.7	2.81	90.0	2.79	90.0	2.80	90.1	
	O1f-O3f	2.58	77.9	2.58	76.4	2.57	76.8	2.59	77.3	<i>f</i>
	O1f-O4c	2.67	84.6	2.66	81.1	2.63	82.0	2.63	82.5	<i>f</i>
	O1f-O5c	3.02	106.5	3.12	108.5	3.01	106.8	3.00	106.4	
	O2f-O3c	2.95	95.4	2.98	96.7	2.89	95.3	2.87	94.4	
	O2f-O3f	2.72	83.0	2.71	82.2	2.66	81.2	2.68	81.6	<i>e</i>
	O2f-O5c	2.84	97.9	2.87	98.5	2.76	96.8	2.76	96.1	
	O3c-O3f	2.59	77.6	2.59	76.4	2.54	76.7	2.53	76.3	<i>e</i>
	O3c-O4c	2.71	83.9	2.73	82.9	2.66	84.0	2.66	84.6	<i>e</i>
	O3c-O5c	2.86	97.9	2.93	98.7	2.84	100.0	2.85	100.3	
	O3f-O4c	2.66	79.5	2.67	78.0	2.65	79.6	2.66	80.0	<i>f</i>
	O4c-O5c	2.93	99.9	3.04	101.6	2.93	102.6	2.93	102.5	
	O1f-O3c		153.8		150.8		151.8		152.3	
	O2f-O4c		162.2		159.7		160.5		161.2	
O3f-O5c		175.5		175.0		175.9		175.7		
Mean	2.78		2.81		2.74		2.75			
V3 octahedra	O1b-O4	2.71	84.2	2.72	84.3	2.67	80.4	2.68	81.2	<i>e</i>
	O1b-O5a	2.97	93.2	2.95	96.8	2.90	90.3	2.86	89.6	
	O1b-O6	2.71	85.9	2.72	84.1	2.69	83.9	2.67	84.6	<i>e</i>
	O1b-O7a	3.01	95.1	2.99	96.4	2.80	90.1	2.76	89.4	
	O4-O5a	2.88	90.0	2.84	90.6	2.72	84.1	2.71	84.3	
	O4-O6	2.83	91.3	2.86	88.1	2.80	89.4	2.78	89.3	
	O4-O10c	2.99	96.4	3.01	95.1	2.91	95.5	2.89	95.4	
	O5a-O7a	2.86	88.1	2.83	91.3	2.72	89.6	2.72	89.5	
	O5a-O10c	2.72	84.1	2.71	85.9	2.68	87.2	2.65	86.6	<i>e</i>
	O6-O7a	2.84	90.6	2.88	90.0	2.81	95.9	2.80	96.0	
	O6-O10c	2.95	96.8	2.97	93.2	2.88	98.1	2.86	98.9	
	O7a-O10c	2.72	84.3	2.71	84.2	2.73	93.8	2.71	93.6	
	O1b-O10c		177.2		177.2		175.4		175.1	
	O4-O7a		177.9		177.9		168.6		168.7	
O5a-O6		178.3		178.3		172.0		172.0		
Mean	2.85		2.85		2.78		2.75			

TABLE V (continued)

	Bonded oxygens	V_3O_5				V_6O_{11}		V_7O_{13}		
		O-O	O-V-O	O-O	O-V-O	O-O	O-V-O	O-O	O-V-O	
V4 octahedra	O2-O3	2.72	84.1	2.71	85.9	2.66	80.7	2.68	80.9	<i>e</i>
	O2-O4	2.86	88.1	2.83	91.3	2.80	85.7	2.82	85.8	
	O2-O7c	2.88	90.0	2.84	90.6	2.65	83.2	2.64	82.0	
	O2-O8c	2.97	93.2	2.95	96.8	2.84	91.7	2.81	90.0	
	O3-O4	2.72	84.3	2.71	84.2	2.66	81.4	2.66	82.2	<i>e</i>
	O3-O7c	2.99	96.4	3.01	95.1	2.86	93.0	2.84	92.7	
	O3-O9c	2.95	96.8	2.97	93.2	2.76	90.4	2.75	90.7	
	O4-O8c	3.01	95.1	2.99	96.4	2.97	98.3	2.91	96.8	
	O4-O9c	2.84	90.6	2.88	90.0	2.94	97.9	2.92	97.7	
	O7c-O8c	2.71	84.2	2.72	84.3	2.59	85.9	2.58	86.4	<i>e</i>
	O7c-O9c	2.83	91.3	2.86	88.1	2.72	92.4	2.74	93.9	
	O8c-O9c	2.71	85.9	2.72	84.1	2.80	97.2	2.81	98.5	
	O2-O9c		178.3		178.3		169.8		170.4	
	O3-O8c		177.2		177.2		172.3		170.8	
	O4-O7c		177.9		177.9		168.3		167.4	
	Mean	2.85		2.85		2.77		2.76		
V5 octahedra	O5b-O8					2.75	87.2	2.73	86.1	
	O5b-O9a					2.87	93.1	2.84	90.8	
	O5b-O10					2.68	83.2	2.65	82.7	<i>e</i>
	O5b-O11a					2.77	88.5	2.75	87.9	
	O8-O9a					2.76	90.6	2.76	90.5	
	O8-O10					2.71	88.0	2.71	88.2	
	O8-O13i					2.80	92.4	2.78	93.7	
	O9a-O11a					2.71	89.2	2.68	88.5	
	O9a-O13i					2.72	88.5	2.67	89.2	<i>e</i>
	O10-O11a					2.79	91.7	2.78	92.2	
	O10-O13i					2.94	97.0	2.86	97.4	
	O11a-O13i					2.77	92.0	2.72	92.3	
	O5b-O13i						179.5		179.8	
	O8-O11a						175.7		173.9	
O9a-O10						174.4		173.4		
	Mean					2.77		2.74		
V6 octahedra	O6-O7					2.78	89.4	2.89	90.0	
	O6-O8					2.74	88.0	2.77	88.7	
	O6-O11c					2.75	89.7	2.74	89.0	
	O6-O12c					2.77	89.7	2.74	89.7	
	O7-O8					2.59	83.0	2.58	82.8	<i>e</i>
	O7-O11c					2.85	95.0	2.85	95.3	
	O7-O13c					2.72	88.8	2.67	86.9	
	O8-O12c					2.89	96.1	2.87	96.1	
	O8-O13c					2.77	91.3	2.77	90.7	
	O11c-O12c					2.62	85.8	2.60	85.8	<i>e</i>
	O11c-O13c					2.73	90.9	2.75	91.4	
	O12c-O13c					2.79	92.1	2.79	93.4	
	O6-O13c						178.1		176.9	
	O7-O12c						178.8		178.9	
O8-O11c						177.0		177.0		
	Mean					2.75		2.74		

TABLE V (continued)

	Bonded oxygens	V_3O_5		V_6O_{11}		V_7O_{13}		
		O-O	O-V-O	O-O	O-V-O	O-O	O-V-O	
V7 octahedra	O9b-O12					2.75	89.7	
	O9b-O12e					2.77	90.3	
	O9b-O13a					2.89	94.7	
	O9b-O13d					2.67	85.3	e
	O9i-O12					2.77	90.3	
	O9i-O12e					2.75	89.7	
	O9i-O13a					2.67	85.3	e
	O9i-O13d					2.89	94.7	
	O12-O13a					2.76	90.9	
	O12-O13d					2.72	89.1	
	O12e-O13a					2.72	89.1	
	O12e-O13d					2.76	90.9	
	O9b-O9i							180.0
	O12-O12e							180.0
O13a-O13d							180.0	
	Mean					2.76		
V8 octahedra	O10-O11					2.78	91.0	
	O10-O11i					2.73	90.0	
	O10-O12					2.76	90.0	
	O10-O12i					2.75	90.0	
	O10i-O11					2.73	89.0	
	O10i-O11i					2.78	91.0	
	O10i-O12					2.75	90.0	
	O10i-O12i					2.76	90.0	
	O11-O12					2.60	84.7	e
	O11-O12i					2.85	95.3	
	O11i-O12					2.85	95.3	
	O11i-O12i					2.60	84.7	e
	O10-O10i							180.0
	O11-O11i							180.0
O12-O12i							180.0	
	Mean					2.74		

The relation of symbols for oxygen atoms between V_7O_{13} and other phases should be referred to Table IV. Standard errors are around 0.02 Å and 0.6° for distances and angles, respectively. *e*, oxygen atoms of shared edges; and *f*, oxygen atoms of shared faces.

factors of V_3O_5 are listed in Table II(a) and those of V_3O_5 (converted into triclinic cell), V_6O_{11} , and V_7O_{13} in Table II(b). The interatomic distances V-O (Table IV), O-O (Table V) and V-V (Table VI) and angles O-V-O (Table V) are given for V_3O_5 , V_6O_{11} , and V_7O_{13} . The distances and angles were calculated by using a version of the program RDA4 of UNICS system (21).

All the computations were carried out by NEAC-700 and FACOM 230-60 computers

at Computation Center Osaka University and Data Processing Center of Kyoto University, respectively.

Discription and discussion of the structure

a. General Features

The structures of V_nO_{2n-1} ($2 \leq n \leq 7$) are constructed by VO_6 octahedra. Oxygen atoms are approximately in the hexagonal close packing.

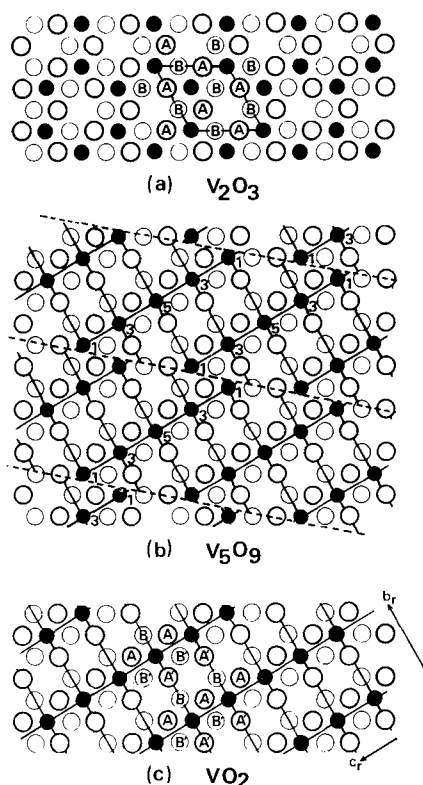


FIG. 1. Parts of the structures of V_2O_3 , V_5O_9 , and VO_2 based upon the hexagonal close packing of oxygen atoms. Open and black circles represent oxygen and vanadium atoms, respectively. A and B show the oxygen atoms with different height. Real lines show a hexagonal corundum-type cell in V_2O_3 and a rutilite-type cell projected along the a_r axis in V_5O_9 and VO_2 .

The structures of V_2O_3 , V_5O_9 , and VO_2 are schematically shown in Fig. 1 with emphasis on the packing layers of the hexagonal close packing of oxygen atoms. The hexagonal unit cell of the corundum-type structure is projected along the c axis (Fig. 1a) and the tetragonal one of the rutilite-type structure is projected along the a_r axis (Fig. 1c). Although A (B) shows the same packing layer in the V_2O_3 structure, A and A' (B and B') are not in the same layer but constitute slightly separate layers in the VO_2 structure.

In the structure of V_5O_9 (Fig. 1b) the part between two parallel dotted lines shows the rutilite-type structure. The unit cells of the rutilite-type structure are shown with real lines. The directions of a_r , b_r , and c_r are the same as

the figure of VO_2 . The VO_6 octahedra of V1, V3, V5, V3, and V1 in V_5O_9 share edges with each other and make a finite straight chain along the c_r axis. Those of V2, V4, V6, V4, and V2 are in the upper plane and at the positions with the magnitude of $\frac{1}{2}b_n$ along b_n ($=a_r + b_r + c_r$) from V1, V3, V5, V3, and V1, respectively. The rutilite-type parts are mutually shifted by a vector of $c_n/(2n-1)$ ($=\frac{1}{2}(b_r + c_r)$) in the boundaries shown by dotted lines which is called "crystallographic shear plane (CSP)" by Wadsley (22).

The end octahedra $V1O_6$ and $V2O_6$ of the straight chains (Fig. 1b) share the faces and edges with the octahedra of $V1O_6$ and $V2O_6$ of the neighboring rutilite-type part and make a infinite double chain running along the b_n axis. This chain is shown along b axes of V_4O_7 and V_5O_9 in Fig. 2, in which perspective views are given almost parallel to the oxygen packing plane for V_4O_7 and V_5O_9 .

In conclusion, there are three kinds of octahedral chain in the structures of V_nO_{2n-1} ($3 \leq n \leq 7$). Two of them are zig-zag chains shared by edges like $\cdots-V5-V3-V1-V1-V3-V5-\cdots$ and $\cdots-V6-V4-V2-V2-V4-V6-\cdots$ (Fig. 1). Another one is an infinite double chain shared by faces and edges like $\cdots-V1-V1-V2-V2-\cdots$ (Fig. 2). The three kinds of chains of V_7O_{13} are shown in Fig. 3. The infinite double chain can be found also in the structure of V_2O_3 .

b. Deviations from the Ideal Structures

The atomic coordinates of V_3O_5 are only slightly different from those by Asbrink et al. (16) based on space group $C2/c$. The directions and magnitudes of shifts from the ideal positions which are shown by + and - and numbers in Table III are essentially identical for all coordinates corresponding to V1, V2, ..., O1, O2, ..., of the series except V_3O_5 . The results for V_4O_7 and V_5O_9 were obtained from those by Marezio et al. (13, 14). The shifts are different in direction for some atoms, however, their absolute values are very small. In the structure of V_3O_5 the x coordinates of V1 atoms of lower-half and upper-half parts are inversely shifted, respectively, and the magnitudes of shifts of V3 and V4 are very

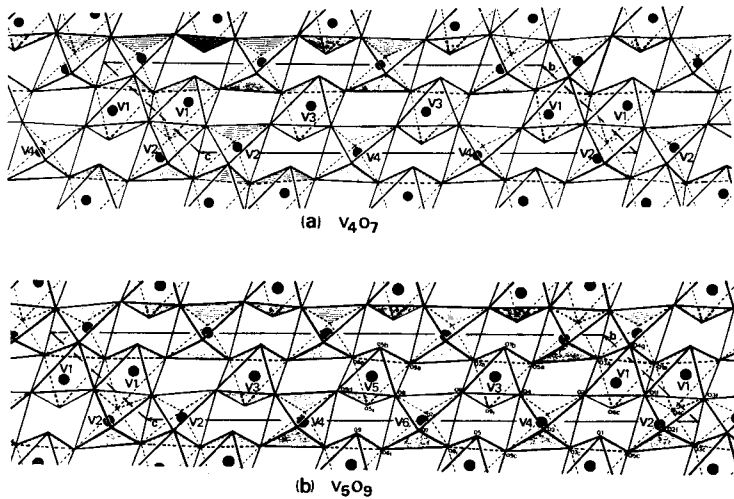


FIG. 2. Perspective views of the structures of V_4O_7 and V_5O_9 based upon the VO_6 octahedra. Black circles show vanadium atoms. Shaded planes are parallel to the packing layers shown in Fig. 1. The b and c axes are shown in the oblique and horizontal directions, respectively.

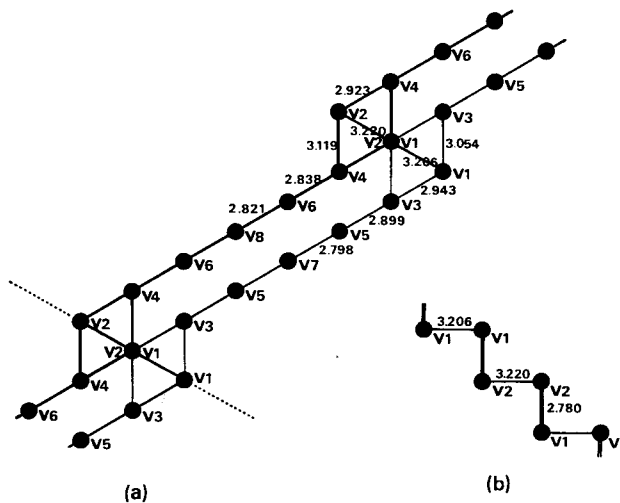


FIG. 3. (a) Arrangements of V atoms in V_7O_{13} . Atoms are projected along the a axis shown in Fig. 1. The even and odd numbered V atoms show the atoms with different height, respectively. (b) Infinite double chain running along the b axis. Double lines show the V-V combinations across the face-shared octahedra.

small and the oxygen atoms have identical tendency of shift with other phases.

The shift from the ideal position is most striking for the V1 and V2 atoms which construct the infinite double chain in the CSP, and becomes gradually less remarkable for the vanadium atoms with greater distances from the CSP. For example in V_7O_{13} , the shifts of V1 and V2 are 0.322 and 0.335 Å,

respectively, and those of V3 and V4 are 0.217 and 0.207 Å, respectively, and so on. Oxygen atoms have the similar tendency of shift to that of vanadium atoms.

c. Interatomic Distances and Angles

The interatomic distances of the oxygen atoms on the shared faces and edges of VO_6 octahedra are generally smaller than those of

the oxygen atoms at the shared corners. On the other hand, the V–O distances of the oxygen atoms at the shared corners are smaller than those of the oxygen atoms on the shared faces and edges. These features are most remarkable with the oxygen atoms in the infinite double chain in the CSP and become less remarkable with those at greater distance from the CSP.

The features of the interatomic distances described above are clear for V_7O_{13} (Tables IV and V). The V1 and V2 octahedra on the CSP share a face of three oxygen atoms of $O1_a$, $O3_a$ and $O4_g$. The distances of $O1_a$ – $O3_a$, $O1_a$ – $O4_g$ and $O3_a$ – $O4_g$ are 2.59, 2.63, and 2.66 Å, respectively. The V1 octahedra is also connected with $V1O_6$ and two $V3O_6$'s by three edges of $O1_a$ – $O1_f$, $O1_a$ – $O6_c$ and $O1_f$ – $O4_g$ with 2.54, 2.67, and 2.68 Å, respectively. On the other hand, other six distances of the oxygen atoms in the shared corners are greater within the range from 2.72 to 2.93 Å. The V3 and V4 octahedra share three edges with neighboring octahedra, and V5, V6, V7, and V8 octahedra share two edges. The shared edges of each octahedron are shorter than the unshared edges.

The O–V–O angles of oxygen atoms on the

shared faces and edges of VO_6 octahedra are also generally smaller than those of oxygen atoms at the shared corners.

The V–V distances across the shared faces in the CSP are largest in V_3O_5 and almost identical in the series from V_4O_7 to V_7O_{13} (Table VI). The distances across the shared edges are largest in the combination of V1 and V2 octahedra and they become gradually smaller in the combinations of octahedra with greater distance from the CSP. The change of the V–V distances are shown in Fig. 3 for V_7O_{13} .

The mean V–O and O–O distances for VO_6 octahedra of V_nO_{2n-1} ($2 \leq n \leq 7$) are listed together with those for VO_2 (Table VII). The mean values for the pairs of the octahedra, V1 and V2, V3 and V4, V5 and V6, and V7 and V8, are classified under OCT1, OCT2, OCT3 and OCT4, respectively, because each pair plays structurally the similar role in all phases.

The mean V–O and O–O distances are relatively larger in OCT2 than other octahedra, and become gradually smaller in the order of OCT1, OCT3 and OCT4. They are much smaller in VO_2 than in other phases. The mean V–O and O–O distances of octa-

TABLE VI

COMPARISON OF THE V–V DISTANCES OF V_nO_{2n-1} ($3 \leq n \leq 7$)

Combinations of V atoms		V_3O_5	$V_4O_7^a$	$V_5O_9^b$	V_6O_{11}	V_7O_{13}	Mean		
Face-sharing octahedra		V1–V2h	2.795	2.795	2.768	2.768	2.774	2.780	2.780
Edge-sharing octahedra	OCT 1	V1–V1h	3.250	3.250	3.202	3.208	3.161	3.206	3.217
		V2–V2j	3.250	3.250	3.189	3.190	3.229	3.220	
	OCT 1–OCT 2	V1–V3c	3.040	2.998	2.930	2.947	2.944	2.943	3.005
		V1–V3g	2.973	2.983	3.009	3.039	3.040	3.054	
	OCT 2–OCT 3	V2–V4c	2.973	2.983	2.964	2.958	2.966	2.923	2.868
		V2–V4f	3.040	2.998	3.066	3.096	3.133	3.119	
	OCT 3–OCT 4	V3–V5c				2.878	2.937	2.899	2.810
		V4–V6c				2.823	2.828	2.838	
			V5–V7c					2.798	
			V6–V8c					2.821	

^{a, b} The distances of V–V for V_4O_7 and V_5O_9 were quoted from Marezio et al. (13, 14). Standard errors for V_3O_5 , V_6O_{11} , and V_7O_{13} are around 0.005 Å.

TABLE VII
COMPARISON OF THE MEAN V-O AND O-O DISTANCES (Å), s_{vO} , s_{OO} , AND s_{OvO}

		V ₂ O ₃ ^a	V ₃ O ₅	V ₄ O ₇ ^a	V ₅ O ₉ ^a	V ₆ O ₁₁	V ₇ O ₁₃	VO ₂ ^a	
								I	II
Mean of V-O	OCT 1	2.010	1.999	1.977	1.969	1.964	1.964	1.937	1.925
	OCT 2		2.018	1.974	1.969	1.967	1.959		
	OCT 3				1.951	1.955	1.942		
	OCT 4						1.947		
Mean of O-O	OCT 1	2.832	2.794	2.765	2.752	2.743	2.744	2.728	2.721
	OCT 2		2.849	2.786	2.776	2.774	2.757		
	OCT 3				2.755	2.762	2.743		
	OCT 4						2.753		
s_{vO}	OCT 1	2.2	5.6	5.8	6.2	6.9	6.9	5.9	0.3
	OCT 2		2.1	3.2	4.2	4.5	5.0		
	OCT 3				1.0	2.2	2.5		
	OCT 4						1.2		
s_{OO}	OCT 1	3.9	5.9	5.4	5.2	5.4	5.1	3.0	3.1
	OCT 2		4.1	3.4	3.5	3.8	3.5		
	OCT 3				2.9	2.8	2.8		
	OCT 4						2.8		
s_{OvO}	OCT 1	6.6	11.7	11.5	11.4	11.7	11.7	6.8	4.0
	OCT 2		5.2	5.4	6.7	6.6	6.5		
	OCT 3				3.5	3.9	4.3		
	OCT 4						3.5		

^a The values were calculated from the interatomic distances and angles by following references: V₂O₃, Dernier (23); V₄O₇, Marezio et al. (13) for V-O, O-O, s_{vO} and s_{OO} , Horiuchi et al. (10) for s_{OvO} ; V₅O₉, Marezio et al. (14) for V-O, O-O, s_{vO} , and s_{OO} , Horiuchi et al. (10) for s_{OvO} ; VO₂ I (low temperature form), Longo and Kierkegaard (24); VO₂ II (high temperature form), McWhan et al. (25).

hedra change with the volume of the octahedra. Thus, the value of $v_n/(2n-1)$, where v_n is the unit cell volume of V_nO_{2n-1}, is greater in the phase with smaller n values, because the OCT1 or OCT2 occupy a greater part of the whole structure in the phase with smaller n values. This result is in good agreement with that given by Horiuchi et al. (5).

d. Characteristics of VO₆ Octahedra

It is of interest to note that the arrangements of oxygen atoms for VO₂ is denser than V₂O₃,

though oxygen atoms of V₂O₃ arrange close to the ideal hexagonal close-packing and those of VO₂ a distorted hexagonal close-packing. This apparent conflict takes place because the size of octahedra is affected by the strong V-V interactions across the shared faces and edges especially in OCT1 and OCT2.

The octahedral configuration of oxygen atoms around vanadium atoms is also affected by the strong V-V interactions in the CSP. This effect is expressed quantitatively by s_{OO} , s_{vO} and s_{OvO} which are defined by the following equations:

$$s_{00} = \frac{100}{\bar{A}} \cdot \left[\frac{\sum_{i=1}^{12} (A_i - \bar{A})^2}{11} \right]^{1/2}$$

$$s_{v0} = \frac{100}{\bar{B}} \cdot \left[\frac{\sum_{i=1}^6 (B_i - \bar{B})^2}{5} \right]^{1/2}$$

$$s_{0v0} = \frac{100}{90} \cdot \left[\frac{\sum_{i=1}^{12} (C_i - 90)^2}{11} \right]^{1/2},$$

where A_i , B_i , and C_i are the O-O, V-O distances and O-V-O angles in each octahedra, respectively, \bar{A} and \bar{B} are their mean values, and summations in the equations are calculated for all combinations of O-O, V-O, and O-V-O in each octahedron. The parts of the square roots in the equations, are the standard deviations of the distances of O-O and V-O and angles of O-V-O for each VO_6 octahedron (26). The values of s_{00} , s_{v0} , and s_{0v0} are the standard deviations which are multiplied by 100 and divided by their mean values. The values of s_{00} , s_{v0} , and s_{0v0} are listed (Table VII). The values of s_{00} are effectively influenced by the distortion from the regular oxygen octahedron, and s_{v0} and s_{0v0} , by both distortion and displacement of vanadium atoms from the centers of the oxygen octahedra.

The change of s_{00} , s_{v0} , and s_{0v0} is most remarkable in the octahedra (OCT1) of the CSP. The distortion becomes less remarkable with the distances from the CSP. The values of s_{00} become slightly smaller and those of s_{v0} and s_{0v0} become greater for the phase with larger n values. This tendency is more remarkable in the OCT1 and in the octahedra nearer to the CSP.

Thus, when the part of the rutile-type structure is wide as in V_6O_{11} or V_7O_{13} , the structural characteristics are represented by smaller expansion and distortion of oxygen octahedra and by greater displacement of vanadium atoms from the centers of octahedra. On the other hand, when the part of rutile-type structure is narrow as in V_3O_5 or V_4O_7 , the structural characteristics are represented by greater expansion and distortion of octahedra and smaller displacement of vanadium atoms. The displacement of vanadium

atoms from the centers of octahedra and the distortion of octahedra are small in the structure of V_2O_3 and the high temperature form VO_2 in comparison with the octahedra in the CSP (OCT1) of V_nO_{2n-1} ($3 \leq n \leq 7$). In the low-temperature form VO_2 , however, great displacement of vanadium atoms is observed though the distortion of octahedra is small. The features of octahedra (OCT1) of V_nO_{2n-1} ($3 \leq n \leq 7$) at the CSP are quite different from those of V_2O_3 , though both octahedra construct an infinite double chain shared by faces and edges in their structures. The structural characteristics of octahedra with greater distance from the CSP are, however, more similar to those of high temperature form VO_2 .

Acknowledgments

The authors wish to thank Dr. K. Nagasawa, Professor T. Takada and Dr. Y. Bando of the Institute for Chemical Research, Kyoto University for kindly providing the single crystals of V_nO_{2n-1} .

References

1. A. MAGNELI, *Acta Chem. Scand.* **2**, 501 (1948).
2. G. ANDERSSON, *Acta Chem. Scand.* **8**, 1599 (1954).
3. S. ANDERSSON, *Acta Chem. Scand.* **14**, 1161 (1960).
4. S. ANDERSSON AND L. JAHNBERG, *Ark. Kemi* **21**, 412 (1963).
5. H. HORIUCHI, M. TOKONAMI, N. MORIMOTO, K. NAGASAWA, Y. BANDO, AND T. TAKADA, *Mat. Res. Bull.* **6**, 833 (1971).
6. K. NAGASAWA, *Mat. Res. Bull.* **6**, 853 (1971).
7. RALPH W. G. WYCKOFF, "Crystal Structures," 2nd ed., Vol. 1, pp. 250, Wiley-Interscience, New York (1963).
8. S. ASBRINK, *Mat. Res. Bull.* **6**, 861 (1975).
9. H. HORIUCHI, M. TOKONAMI, N. MORIMOTO, AND K. NAGASAWA, *Acta Cryst.* **B28**, 1404 (1972).
10. H. HORIUCHI AND N. MORIMOTO, *Acta Cryst.* **A28**, S55 (abst.) (1972).
11. M. MAREZIO, P. D. DERNIER, D. B. MCWHAN, AND J. P. REMEIK, *Mat. Res. Bull.* **5**, 1015 (1970).
12. M. MAREZIO, D. B. MCWHAN, P. D. DERNIER, AND J. P. REMEIK, *J. Solid State Chem.* **6**, 213 (1973).
13. M. MAREZIO, D. B. MCWHAN, P. D. DERNIER, AND J. P. REMEIK, *J. Solid State Chem.* **6**, 419 (1973).
14. M. MAREZIO, P. D. DERNIER, D. B. MCWHAN, AND S. KACHI, *J. Solid State Chem.* **11**, 301 (1974).
15. S. WESTMAN, *Acta Chem. Scand.* **15**, 217 (1961).

16. S. ASBRINK, S. FRIBERG, A. MAGNELI, AND G. ANDERSSON, *Acta Chem. Scand.* **13**, 603 (1959).
17. T. FUKAMACHI, *Tech. Rep., ISSP, B*, **12**, 1 (1971).
18. M. TOKONAMI, *Acta Cryst.* **19**, 486 (1965).
19. W. H. ZACHARIASEN, *Acta Cryst.* **16**, 1139 (1963).
20. W. R. BUSING, K. O. MARTIN, AND H. A. LEVY. "Program ORFLS, Report ORNL-TM-305," Oak Ridge National Laboratory, Oak Ridge, Tennessee (1962).
21. T. SAKURAI, Universal Cryst. Comput. Prog. Sys. (UNICS), Cryst. Soc. of Japan (1967).
22. A. D. WADSLEY, *Rev. Pure Appl. Chem.* **5**, 165 (1955).
23. P. D. DERNIER, *J. Phys. Chem. Solids* **31**, 2569 (1970).
24. J. M. LONGO AND P. KIERKEGAARD, *Acta Chem. Scand.* **24**, 420 (1970).
25. D. B. MCWHAN, M. MAREZIO, J. P. REMEIKA, AND P. D. DERNIER, *Phys. Rev. B* **10**, 490 (1974).
26. K. ROBINSON, G. V. GIBBS, AND P. H. RIBBE, *Science* **172**, 567 (1971).